



## Organic contaminants degradation by modification carbon felt derived from Mn, Fe layered double hydroxide cathode

Bui Nguyen Thu Ha<sup>1,2</sup>, Phan Quang Thang<sup>3</sup>, Nguyen Nhat Huy<sup>4,5</sup>, Nguyen Tien Loi<sup>6</sup>,  
Nguyen Quang Vinh<sup>6</sup>, Nguyen Trung Dung<sup>6,\*</sup>

<sup>1</sup> Graduate University of Science and Technology, Vietnam Academy of Science and Technology, 18 Hoang Quoc Viet, Nghia Do Ward, Hanoi, Vietnam.

<sup>2</sup> Faculty of Land Management, Hanoi University of Natural Resources and Environment, 41A Phu Dien, Phu Dien Ward, Hanoi, Vietnam

<sup>3</sup> Institute of Science and Technology for Energy and Environment (ISTEE), Vietnam Academy of Science and Technology (VAST), 18 Hoang Quoc Viet, Nghia Do Ward, Hanoi, Vietnam

<sup>4</sup> Faculty of Environment and Natural Resources, Ho Chi Minh City University of Technology (HCMUT), 268 Ly Thuong Kiet Street, Dien Hong Ward, Ho Chi Minh City, Vietnam

<sup>5</sup> Vietnam National University Ho Chi Minh City, Linh Trung Ward, Thu Duc City, Ho Chi Minh City, Vietnam

<sup>6</sup> Faculty of Physics and Chemical Engineering, Le Quy Don Technical University, 236 Hoang Quoc Viet, Nghia Do Ward, Hanoi, Vietnam

\*Email: ntduong@lqdtu.edu.vn

### ARTICLE INFO

Received: 03/08/2025

Accepted: 03/09/2025

Published: 30/09/2025

### Keywords:

Layered double hydroxide;  
Mn, Fe; Dye; antibiotics;  
carbon felt; electro Fenton

### ABSTRACT

The traditional electro-Fenton (EF) process faced significant challenges, including a narrow pH range and poor catalyst reusability. The heterogeneous electro-Fenton (EF) process was a promising wastewater treatment technology because it generated H<sub>2</sub>O<sub>2</sub> in situ and operated over a wide pH range without producing metal sludge. In this study, Mn-Fe layered double hydroxide (MnFe-LDH) electrodes were fabricated on carbon felt by an in situ hydrothermal method and were applied as cathodes for the heterogeneous electro-Fenton process to degrade organic pollutants, including antibiotics (oxytetracycline, levofloxacin, ciprofloxacin) and tartrazine dye. The surface morphology and structure of the catalyst were analysed by scanning electron microscopy (SEM), energy-dispersive X-ray spectroscopy (EDX), X-ray diffraction (XRD), Fourier-transform infrared spectroscopy (FT-IR), and contact angle measurements. The results showed that 58.45–96.01% of the pollutants were decomposed under natural pH conditions after 120 minutes at a current intensity of 24 mA, pollutant concentration of 10 mg/L, and 50 mM Na<sub>2</sub>SO<sub>4</sub> as the electrolyte. The MnFe-LDH/CF cathode demonstrated high durability and reusability. It could be applied in the electro-Fenton process to remove organic pollutants that were difficult to biodegrade in aqueous environments.

### Introduction

Water pollution from organic contaminants such as antibiotics and dyes has become a global concern [1].

Antibiotics, including levofloxacin, ciprofloxacin, and oxytetracycline, are widely detected in aquatic environments due to discharges from healthcare, pharmaceuticals, and animal or human excretions [2].

Their persistence promotes bacterial resistance, microbial proliferation, and the emergence of new pathogens, posing serious public health risks. Similarly, tartrazine, a commonly used azo dye in food, cosmetics, and pharmaceuticals, is linked to carcinogenicity and adverse health effects such as urticaria, asthma, mutagenicity, and phototoxicity. These pollutants are poorly biodegradable and are inefficiently removed by conventional treatments such as coagulation, biological oxidation, adsorption, ion exchange, and chemical oxidation [3, 4].

Homogeneous Fenton processes can mineralize such pollutants into  $\text{CO}_2$ ,  $\text{H}_2\text{O}$ , and inorganic ions, but are limited by strict acidic conditions (pH 2–4) and generate large amounts of iron sludge[5]. Heterogeneous electro-Fenton (EF) technology has emerged as a promising alternative due to in situ  $\text{H}_2\text{O}_2$  generation, strong hydroxyl radical production, high removal efficiency, and catalyst reusability[6]. Cathode materials are particularly critical as they influence  $\text{H}_2\text{O}_2$  formation, pH range, sludge reduction, and overall electrochemical efficiency[7]. Carbon-based materials (e.g., carbon felt, graphite felt, graphite, activated carbon fibers) are widely applied because of their excellent conductivity, mechanical strength, and corrosion resistance [8, 9].

Carbon felt (CF), which was used as a cathode for heterogeneous electrochemical Fenton, had many advantages. However, due to its hydrophobic surface properties and poor redox reaction kinetics, CF was modified with catalysts before being applied in a heterogeneous electrochemical Fenton system. Layered double hydroxide (LDH) was a two-dimensional anionic layered material with the general formula  $[(\text{M}^{2+})_{1-x}(\text{M}^{3+})_x(\text{OH})_2]_x^+(\text{A}_{m-x}/m).\text{nH}_2\text{O}$ , where  $\text{M}^{2+}$  and  $\text{M}^{3+}$  represented divalent ( $(\text{Mn}^{2+}, \text{Fe}^{2+}, \text{Co}^{2+}, \text{Mn}^{2+}, \text{Ni}^{2+}, \text{Cu}^{2+}$  or  $\text{Zn}^{2+}$ ) and trivalent ( $\text{Fe}^{3+}, \text{Al}^{3+}, \text{Cr}^{3+}, \text{La}^{3+}$ ) metal ions, respectively. In this formula,  $\text{M}^{3+}/(\text{M}^{2+} + \text{M}^{3+})$  represents the ratio, and  $\text{A}^{m-}$  was the interlayer anion. [10]. LDHs were widely used in electrocatalysis because they had a simple structure and fabrication process, tunable chemical composition, high specific surface area, and environmental friendliness.

Among transition metals, Mn and Fe are abundant, environmentally benign, and catalytically active via redox cycling. Their synergistic incorporation in bimetallic LDHs enhances conductivity and surface reaction kinetics [11, 12]. Although MnFe-LDHs prepared by co-precipitation have shown promise in peroxyomonosulfate (PMS) activation-based AOPs [13, 14], their use in powder form limits recovery and reuse. Hence, developing immobilized MnFe-LDH with high activity and easy separation is crucial for practical water treatment.

In this study, MnFe-LDH/CF cathode was fabricated by hydrothermal method and used for electrochemical degradation of antibiotics and dyes in heterogeneous electrochemical Fenton process. The characteristic properties of the electrodes were analyzed by modern techniques such as SEM, EDX, XRD, FT-IR and contact angle. Initially, the applicability of the electrodes for degradation of different pollutants, reuse and influence of different types of water were evaluated.

## Experimental

### Chemicals and reagents

The chemicals used are all of high purity and do not require purification:  $\text{HNO}_3$  63–65%, Manganese(II) chloride tetrahydrate ( $\text{MnCl}_2 \cdot 4\text{H}_2\text{O}$  98%); Iron(III) chloride hexahydrate ( $\text{FeCl}_3 \cdot 6\text{H}_2\text{O}$  99%); Ammonium Fluoride ( $\text{NH}_4\text{F}$  99%); Urea ( $(\text{NH}_2)_2\text{CO}$  98%); Tartrazine (TTZ) ( $\text{C}_{16}\text{H}_9\text{N}_4\text{Na}_3\text{O}_9\text{S}_2$  97%), Levofloxacin (LFX) ( $\text{C}_{18}\text{H}_{20}\text{FN}_3\text{O}_4$ , 98%), Ciprofloxacin (CFX) ( $\text{C}_{17}\text{H}_{18}\text{FN}_3\text{O}_3$ , 97%), oxytetracycline (OTC) ( $\text{C}_{22}\text{H}_{24}\text{N}_2\text{O}_9$ , 98%) provided by Sigma (USA). Ethanol (99%) was purchased from Duc Giang Chemical Company (Vietnam). Carbon felt (CF) was supplied by Hebei Xingshi New Material Technology Co., Ltd. (China). To investigate the degradation performance of LFX in real water sources, tap water was collected from the campus of Le Quy Don Technical University, while river and lake water were taken from the To Lich River and Nghia Do Lake (Hanoi, Vietnam), and used in the experiments.

### Preparation of MnFe-LDH/CF electrodes

Commercial carbon felt (CF) from China was cut into pieces with a length of 4 cm, a width of 3 cm, and a thickness of 0.5 cm. The CF electrodes were activated by a chemical method as reported in our previous study [15]. The CF electrodes (4 cm  $\times$  3 cm  $\times$  0.5 cm) were immersed in concentrated  $\text{HNO}_3$  for 6 h at room conditions. They were then rinsed with distilled water and ultrasonically cleaned with distilled water (two times), ethanol, acetone, and distilled water (two times) for 15 min each. The electrodes were dried at 80 °C for 12 h and weighed.

The MnFe-LDH/CF electrodes were synthesized by a hydrothermal method (Figure 1). Specifically, 2.474 g  $\text{MnCl}_2 \cdot 4\text{H}_2\text{O}$  (12.5 mmol), 6.757 g  $\text{FeCl}_3 \cdot 6\text{H}_2\text{O}$  (25 mmol), 4.633 g  $\text{NH}_4\text{F}$  (125 mmol), and 15 g urea (250 mmol) were dissolved in 60 mL of double-distilled water. The solution was stirred for 30 min until complete dissolution and was transferred into a Teflon vessel containing three pre-activated CF electrodes. The electrodes were immersed for 60 min and then treated hydrothermally

at 120 °C for 12 h. The obtained electrodes were cooled to room temperature, rinsed repeatedly with distilled water and ethanol, and dried at 80 °C for 12 h.

### Characterization

The morphology of the MnFe-LDH/CF electrodes was characterized by scanning electron microscopy (SEM, JEOL JSM-IT 800) at an accelerating voltage of 30 kV. The crystalline phase composition of MnFe-LDH was analysed by X-ray diffraction (XRD, Bruker D8 Advance) with a wavelength of 1.5406 Å and a 2θ scanning range of 2–80°. Fourier transform infrared spectroscopy (ATR-FTIR, Perkin Elmer) in the range of 4000–400 cm<sup>-1</sup> with a resolution of 4 cm<sup>-1</sup> was used to detect the functional groups of the samples. The elemental composition of the material was determined by energy-dispersive X-ray spectroscopy (EDX, EMSA/MAS Spectral Data File). The wettability of the electrodes was measured by contact angle analysis (DSA25S, KRUSS).

### Fenton electro process

Electrolysis experiments were conducted at room temperature in a 500 mL glass beaker. The current and voltage were controlled by a DC power supply (QJE QJ3003XE, China). The cathode was MnFe-LDH/CF with 4 cm × 3 cm × 0.5 cm dimensions. The anode was a Pt/Ti mesh with dimensions of 10 cm × 5 cm and was rolled lengthwise. The distance between the electrodes was 2.0 cm.

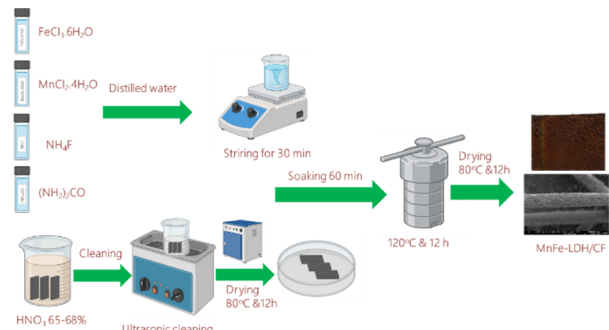


Fig 1: Synthesis of MnFe-LDH/CF electrodes

A total of 250 mL of solution containing 10 mg/L LFX, CFX, OTC, and TTZ with 50 mM Na<sub>2</sub>SO<sub>4</sub> as the electrolyte was prepared. The solution was magnetically stirred at 500 rpm and continuously aerated for 15 min before the EF process started. The current intensity was set at 24 mA.

Every 15 min, 3.00 mL of the solution was withdrawn to measure the absorbance at 290 nm, 275 nm, 355 nm, and 425 nm for LFX, CFX, OTC, and TTZ, respectively. To evaluate electrode reusability, the electrodes were

washed with double-distilled water and ethanol, dried at 80 °C for 12 h, and reused in the next run following the same procedure. The pollutant removal efficiency was determined using the following formula:

$$H (\%) = (1 - \frac{C_t}{C_o}) \cdot 100 = (1 - \frac{A_t}{A_o}) \cdot 100$$

Here, C<sub>o</sub> and A<sub>o</sub> represent the initial concentration and absorbance of the pollutant, while C<sub>t</sub> and A<sub>t</sub> denote the concentration and absorbance at time t.

## Results and discussion

### Characterization of MnFe-LDH/CF

The morphology of the prepared electrode materials was described (Figures 2). The SEM image of raw CF showed a fibrous and fine structure with a fiber diameter of about 10–15 μm (Figure 2a). This structure made the fixation of materials on the surface of raw CF less effective. The CF was chemically treated with concentrated HNO<sub>3</sub> (65–68%) to obtain activated CF. The SEM image showed shallow grooves along the fiber axis, which improved surface adhesion (Figure 2b). The treatment also reduced impurities attached to the CF surface [16].

The SEM image showed that the material was densely distributed on the CF fibers (Figures 2c–d). The MnFe-LDH particles were spherical or rice grain-shaped with needle-like structures and tended to agglomerate (Figure 2d). Voids were observed around the CF, which favored H<sub>2</sub>O<sub>2</sub> formation. These features promoted the Fenton-like process and were consistent with previous reports [9].

The elemental composition of MnFe-LDH/CF was analysed by EDX spectroscopy (Figure 2e). The EDX spectrum showed characteristic signals of Fe, Mn, C, and O elements in the MnFe-LDH/CF material (Figure 2e). All elements were detected with corresponding weight percentages of 9.6% (Fe), 6.8% (Mn), 62.1% (O), and 21.6% (C). No other elements were observed in the EDX spectrum. These results indicate that the synthesized material is of high purity and that the applied method is highly effective in controlling the elemental composition.

The crystallinity and surface functional groups of MnFe-LDH/CF were analyzed by XRD and FTIR (Figures 2f–g). As shown in Figure 2f, the XRD pattern of CF exhibits broad characteristic peaks at 25° and 43.2°, corresponding to the (002) and (100) crystal planes of CF [6]. The XRD pattern of MnFe-LDH/CF showed diffraction peaks at 2θ = 12.31°, 17.31°, 27.45°, 31.7°, 34.68°, 35.52°, 39.55°, 46.74°, and 56.51°. These peaks were characteristic of MnFe-LDH and were consistent with previous studies [11, 17, 18]. Broad peaks of carbon materials were also observed at 2θ = 23.92–26.78°. This

result confirmed the successful synthesis of MnFe-LDH on carbon felt.

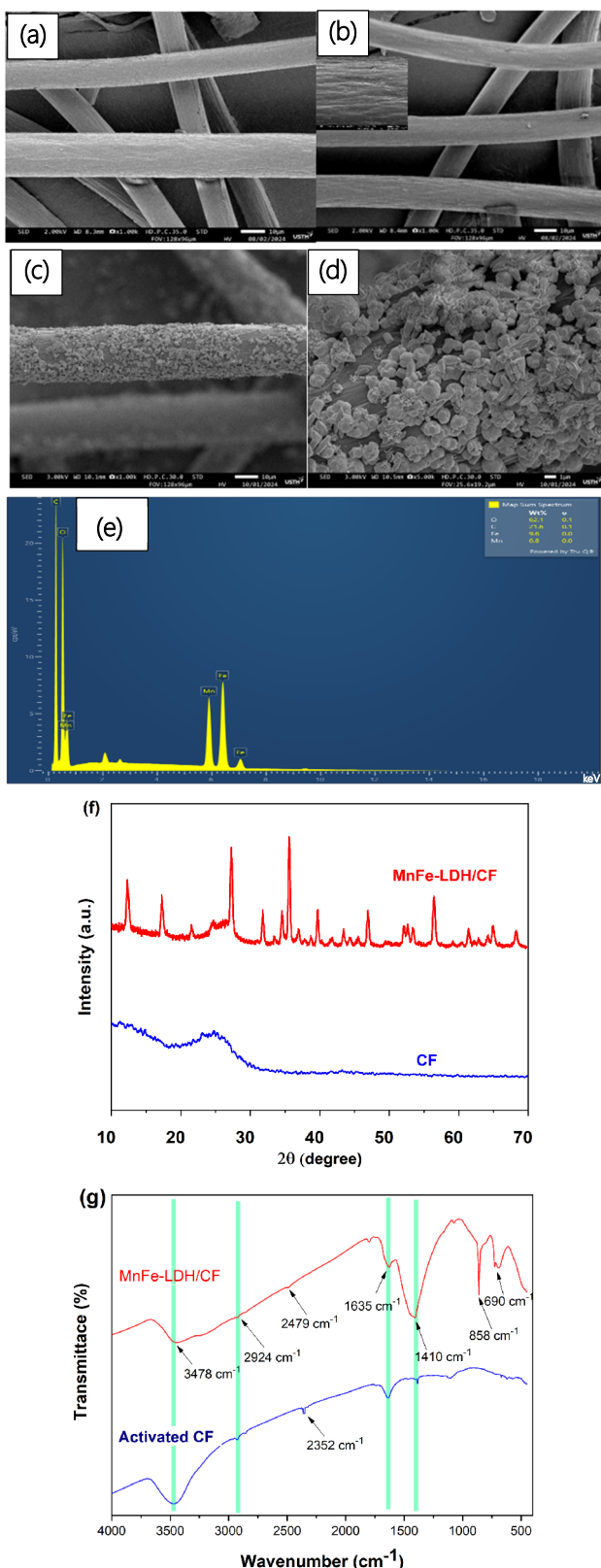


Fig 2: (a). SEM images of raw CF, (b) HNO<sub>3</sub> modification CF, (c,d) SEM images of MnFe-LDH/CF, (e) EDS pattern, (f) XRD pattern of CF and MnFe-LDH/CF, (g) FT-IR pattern of activated CF and MnFe-LDH/CF

<https://doi.org/10.62239/jca.2025.40>

The FTIR spectra of activated CF and MnFe-LDH/CF were measured using the KBr pellet method (Figure 2g). The activated CF spectrum showed absorption bands at 3600–3200 cm<sup>-1</sup> corresponding to hydroxyl stretching vibrations. An absorption band at 1635 cm<sup>-1</sup> was attributed to C=O stretching in carbonyl or ester groups. The absorption bands at 2924 and 2352 cm<sup>-1</sup> confirm the presence of nitrogen functional groups on the activated carbon felt. This result suggested that nitric acid oxidation introduced nitrogen functional groups onto the surface [19]. The FTIR spectrum of MnFe-LDH/CF showed a broad band at 3600–3200 cm<sup>-1</sup> attributed to O-H stretching vibrations of water and hydroxyl groups. A small band at 1635 cm<sup>-1</sup> was assigned to bending vibrations of interlayer and adsorbed water molecules. The peak at 1410 cm<sup>-1</sup> is attributed to the vibrations of intercalated CO<sub>3</sub><sup>2-</sup> ions [20]. In addition, the absorption bands at 858 and 690 cm<sup>-1</sup> were characteristic of Mn–O and Fe–O bonds [11]. These results confirmed the successful coating of MnFe-LDH on the CF substrate.

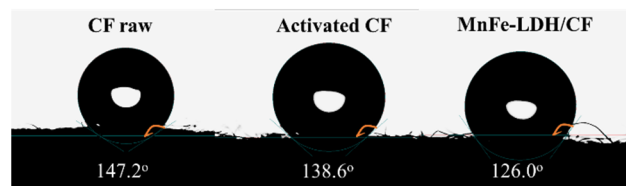


Fig 3: Images of the contact angle of the corresponding cathodes

The contact angle was an important parameter for evaluating the hydrophilic or hydrophobic properties of material surfaces. In the EF system, the hydrophilic property of cathode materials played a key role in absorbing and diffusing the reaction solution. This property directly affected the treatment efficiency. A small contact angle indicated a highly hydrophilic surface, which promoted diffusion and mass transfer. In contrast, a large contact angle indicated a hydrophobic surface, which limited wettability and reduced interactions between the electrode and solution.

The contact angle was measured to evaluate cathode materials' hydrophilic or hydrophobic properties (Figure 3). The raw CF showed a contact angle of 147.2°, indicating a highly hydrophobic surface. This hydrophobicity could limit the contact between the electrolyte and pollutants with the electrode surface, reducing EF efficiency. The activated CF had a contact angle of 138.6°, which indicated reduced hydrophobicity. This result suggested that activation introduced surface functional groups or increased surface roughness, making the surface less

hydrophobic. This improvement enhanced pollutant adsorption and mass transfer during the reaction.

The MnFe-LDH/CF showed a contact angle of 126.0°, which was lower than the other two samples. This result indicated a more hydrophilic surface. The coating of MnFe-LDH likely introduced additional functional groups or modified the surface structure, increasing wettability. Higher hydrophilicity improved contact between the electrode and solution and enhanced hydroxyl radical generation in the EF system [11].

#### Organic contaminants degradation efficiency by MnFe-LDH/CF electrode

The potential for wide application was an important indicator for evaluating the practical value of an electrode. For this reason, the catalytic performance of the electrode was tested for the oxidative degradation of typical toxic organic pollutants, including antibiotics Levofloxacin (LFX), Ciprofloxacin (CIP), Oxytetracycline (OTC) and the dye Tartrazine (TTZ). All degradation experiments were conducted under identical conditions without pH adjustment, following the procedure described in Section 2.

The results showed that after 120 min of treatment, the pollutant removal efficiency decreased in the following order: TTZ (96.01%) > LFX (77.37%) > CFX (71.37%) > OTC (58.48%) (Figure 4). The different degradation efficiencies of the pollutants could be attributed to variations in their molecular structures and the selectivity of hydroxyl radicals for functional groups.

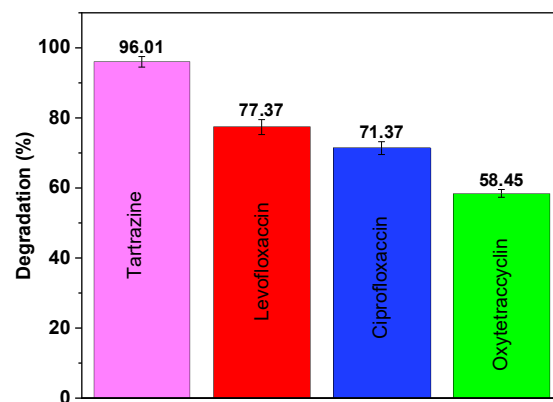


Fig 4: Degradation efficiency of Tartrazine, Levofloxacin, Ciprofloxacin, Oxytetracycline.

The MnFe-LDH/CF cathode achieved 77.37% LFX degradation within 120 min under neutral pH (Table 1), demonstrating high efficiency in environmentally relevant conditions. Unlike many reported systems requiring acidic media or high current, our material operates effectively under mild conditions, underscoring its practical applicability.

The durability and reusability of the MnFe-LDH/CF electrode in the EF process were evaluated using the degradation efficiency of LFX antibiotics. After three reaction cycles, the LFX removal efficiency decreased slightly. The third cycle achieved 70.74%, only 6.63% lower than the first cycle (Figure 5a). This result showed that the MnFe-LDH/CF electrode had good durability and reusability. It was considered a potential material for antibiotic treatment in water environments.

Table 1. Efficiency of LFX degradation by the EF process using different cathodes

Cathode	Experimental conditions of the EF process	Efficiency of Levofloxacin degradation	References
MnFe-LDH/CF	Anode: Pt/Ti, [LFX] = 10mg/L Current intensity = 24mA Neutral pH, $[\text{Na}_2\text{SO}_4]$ =50mM Anode: Pt, [LFX]=20 mg/L Voltage=3V, pH=3.0 $[\text{Na}_2\text{SO}_4]$ =50mM	77.37% degradation of LFX within 120 min	This study
Mn doped $\text{Fe}_3\text{O}_4$ @GF	Anode: Ti/RuO <sub>2</sub> -IrO <sub>2</sub> (DSA) [LFX]=50 mg/L Current intensity =200mA pH=3.0, $[\text{Na}_2\text{SO}_4]$ =50mM	98.9 % degradation of LFX within 120 min	[20]
N doped GF-10	Anode: Pt, [LFX]=15 mg/L Voltage= 1.5V, pH=6.8 $[\text{Na}_2\text{SO}_4]$ =50mM	92 % degradation of LFX within 480 min	[21]
CuFeV LDH@GF	Anode: Pt, [LFX]=15 mg/L Voltage= 1.5V, pH=6.8 $[\text{Na}_2\text{SO}_4]$ =50mM	81.6% degradation of LFX within 120 min	[22]
GF-9	Anode: Pt plate [LFX]:80 mg/L Applied current density = 8 mA/cm <sup>2</sup> pH=3, $[\text{Na}_2\text{SO}_4]$ =50mM	Complete removal of LFX within 60 min	[23]
$\text{V}_2\text{O}_5 \cdot 3\text{H}_2\text{O}$ /N1-GF	[LFX]=5 mg/L, Voltage=0.65V pH=6.8, $[\text{Na}_2\text{SO}_4]$ =100mM	85% degradation of LFX within 60 min	[24]

The degradation of pollutants in the EF system using different water qualities was also evaluated (Figure 5b). The MnFe-LDH/CF electrode decomposed LFX in distilled water and tap water with almost unchanged efficiency. However, the LFX degradation efficiency decreased sharply in Nghia Do Lake water (50.38%) and was strongly inhibited of To Lich River water. This result was likely due to the presence of complex inorganic anions (especially  $\text{Cl}^-$ ) and dissolved organic matter. These components competed with LFX molecules during the degradation process and reduced the removal efficiency [25, 26].

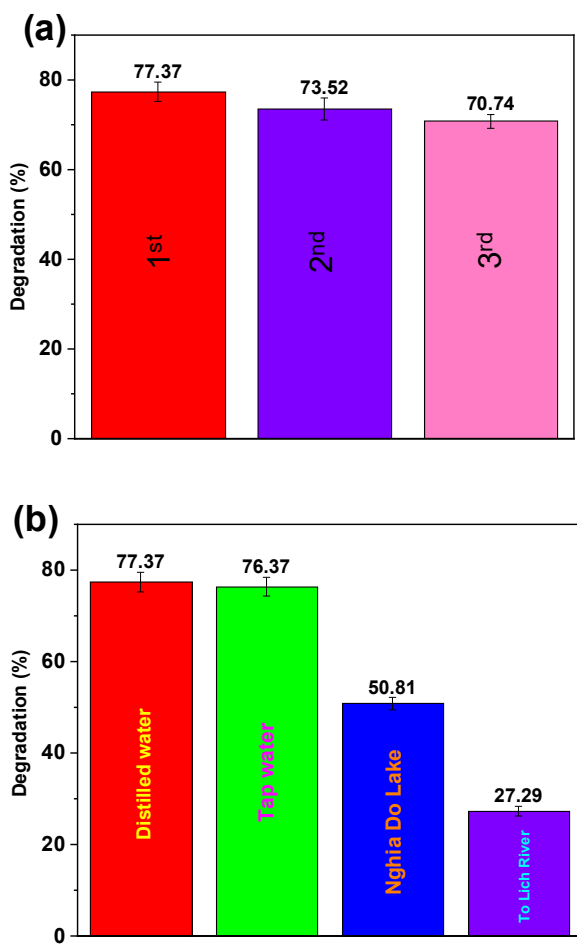


Fig 5: Levofloxacin degradation efficiency (a) after 3 cycles, (b) various water bodies. Reaction conditions: Cathode MnFe-LDH/CF; Anode: Ti/Pt;  $[\text{LFX}] = 10 \text{ mg/L}$ ;  $[\text{Na}_2\text{SO}_4] = 50 \text{ mM}$ ; neutral pH; current intensity = 24mA;  $T^\circ = 25^\circ\text{C}$

### Acknowledgement

This research is funded by the Vietnam National Foundation for Science and Technology Development (NAFOSTED) under grant number 104.05-2024.24

<https://doi.org/10.62239/jca.2025.40>

### Conclusion

In this study, the MnFe-LDH/CF cathode electrode was synthesized by combining CF surface activation with the hydrothermal method. The cathode properties were analysed using SEM, EDX, XRD, FTIR, and contact angle techniques. The results showed that under a current intensity of 24 mA, unadjusted pH, pollutant concentration of 10 mg/L, and 50 mM  $\text{Na}_2\text{SO}_4$  electrolyte, the synthesized material degraded various antibiotics and dyes, including oxytetracycline, levofloxacin, ciprofloxacin, and tartrazine, with removal efficiencies ranging from 58.45% to 96.01%. After three reuse cycles, the treatment efficiency slightly decreased to 70.74%. This study initially provided an effective and environmentally friendly method for treating water pollutants. The proposed MnFe-LDH/CF cathode had the potential to remove recalcitrant pollutants. It was considered a promising EF process for practical applications in large-scale wastewater treatment.

### References

1. N.T. Dung, N.T.C. Tien, P.T. Thu, V.D. Thao, N.P. Thao, P.T. Thuy, L.V. Ngan, N.T. Thuy, K.-Y.A. Lin, N.N. Huy, *Nanotechnol. Environ. Eng.*, 10 (2025) 65. <https://doi.org/10.1007/s41204-025-00464-2>
2. M. Adnan, Z. Zhao, G.A. Ashraf, S. Bashir, B. Teng, J. Yuennan, S.S. Alotaibi, M. Mushtaq, *J. Water Process Eng.*, 76 (2025) 108260. <https://doi.org/10.1016/j.jwpe.2025.108260>
3. M.C. Santos, V.S. Antonin, F.M. Souza, L.R. Aveiro, V.S. Pinheiro, T.C. Gentil, T.S. Lima, J.P.C. Moura, C.R. Silva, L.E.B. Lucchetti, L. Codognoto, I. Robles, M.R.V. Lanza, *Chemosphere*, 307 (2022) 135763. <https://doi.org/10.1016/j.chemosphere.2022.135763>
4. F. Qiu, Y. Pan, L. Wang, H. Song, X. Liu, Y. Fan, S. Zhang, *Sep. Purif. Technol.*, 330 (2024) 125139. <https://doi.org/10.1016/j.seppur.2023.125139>
5. V.D. Thao, N.T. Hoa, N.T. Thuy, N.T. Vinh, N.T.C. Tien, N.T. Dung, K.-Y.A. Lin, D.T.M. Thanh, N.T. Phuong, T.T. Trang, M.B. Nguyen, N.N. Huy, *J. Environ. Chem. Eng.*, 11 (2023) 109698. <https://doi.org/10.1016/j.jece.2023.109698>
6. N.T. Dung, L.T. Duong, N.T. Hoa, V.D. Thao, L.V. Ngan, N.N. Huy, *Chemosphere*, 287 (2022) 132141. <https://doi.org/10.1016/j.chemosphere.2021.132141>
7. K. Wang, H. Li, Y. Yang, P. Wang, Y. Zheng, L. Song, *Sep. Purif. Technol.*, 304 (2023) 122302. <https://doi.org/10.1016/j.seppur.2022.122302>
8. L. Lin, F. Zhang, X. Hou, L. Wang, W. Wu, L. Wang, Y. Li, H. Xie, *Sep. Purif. Technol.*, 334 (2024) 125982. <https://doi.org/10.1016/j.seppur.2023.125982>
9. X. Wang, C. Xu, Y. Zhu, C. Zhou, Y. Yang, J. Miao, W. Zhou, Z. Shao, *Surf. Interfaces*, 44 (2024) 103820. <https://doi.org/10.1016/j.surfin.2023.103820>

10. N.T. Dung, D.T.H. Ha, V.D. Thao, N.P. Thao, T.D. Lam, P.T. Lan, T.T. Trang, L.V. Ngan, B.D. Nhi, N.T. Thuy, K.-Y.A. Lin, N.N. Huy, *Environ. Sci. Pollut. Res.*, 31 (2024) 26773-26789. <https://doi.org/10.1007/s11356-024-32776-2>
11. M. Xu, J. Wei, X. Chen, G. Pan, J. Li, L. Xing, Y. Zhang, Y. Li, Z. Wang, J. Li, *J. Environ. Chem. Eng.*, 10 (2022) 108409. <https://doi.org/10.1016/j.jece.2022.108409>
12. Z.-H. Xie, H.-Y. Zhou, C.-S. He, Z.-C. Pan, G. Yao, B. Lai, *Chem. Eng. J.*, 414 (2021) 128713. <https://doi.org/10.1016/j.cej.2021.128713>
13. Y. Han, Y. Yang, W. Liu, Y. Hou, C. Wang, J. Shang, X. Cheng, *Front. Environ. Sci. Eng.*, 18 (2023) 9. <https://doi.org/10.1007/s11783-024-1769-6>
14. L. Hou, X. Li, Q. Yang, F. Chen, S. Wang, Y. Ma, Y. Wu, X. Zhu, X. Huang, D. Wang, *Sci. Total Environ.*, 663 (2019) 453-464. <https://doi.org/10.1016/j.scitotenv.2019.01.190>
15. N.T.H. Bui, Q.T. Phan, T.D. Nguyen, *J. Sci. Tech. Sect. Phys. Chem. Eng.*, 3 (2025). <https://doi.org/10.56651/lqdtu.jst.v3.n01.942.pce>
16. Y. Gao, W. Zhu, C. Wang, X. Zhao, M. Shu, J. Zhang, H. Bai, *Electrochim. Acta*, 330 (2020) 135206. <https://doi.org/10.1016/j.electacta.2019.135206>
17. G. Chen, L.-c. Nengzi, B. Li, Y. Gao, G. Zhu, X. Cheng, *Sci. Total Environ.*, 695 (2019) 133963. <https://doi.org/10.1016/j.scitotenv.2019.133963>
18. Y.Q. Almajidi, S.S. Abdullaev, B.G. Alani, E.A.M. Saleh, I. Ahmad, M.F. Ramadan, S.S. Al-Hasnawi, R.M. Romero-Parra, *Int. J. Biol. Macromol.*, 246 (2023) 125566. <https://doi.org/10.1016/j.ijbiomac.2023.125566>
19. X. Li, Y. Hu, D. She, W.-B. Shen, *Sustainability*, 12 (2020) 3986. <https://doi.org/10.3390/su12103986>
20. N.T. Dung, B.M. Thuy, L.T. Son, L.V. Ngan, V.D. Thao, M. Takahashi, S. Maenosono, T.V. Thu, *Environ. Res.*, 217 (2023) 114488. <https://doi.org/10.1016/j.envres.2022.114488>
21. X. Liu, D. Yang, Y. Zhou, J. Zhang, L. Luo, S. Meng, S. Chen, M. Tan, Z. Li, L. Tang, *Chemosphere*, 182 (2017) 306-315. <https://doi.org/10.1016/j.chemosphere.2017.05.035>
22. R. Keyikoğlu, A. Khataee, Y. Yoon, *Chemosphere*, 340 (2023) 139817. <https://doi.org/10.1016/j.chemosphere.2023.139817>
23. J.-M. Liu, Z.-Y. Ji, Y.-B. Shi, P. Yuan, X.-F. Guo, L.-M. Zhao, S.-M. Li, H. Li, J.-S. Yuan, *Environ. Pollut.*, 266 (2020) 115348. <https://doi.org/10.1016/j.envpol.2020.115348>
24. S. Fan, Y. Hou, J. Liang, T. Zhu, S. Zhang, T. Liang, J. Pan, Y. Shen, Z. Yu, H. Zhu, S. Wang, *J. Environ. Chem. Eng.*, 12 (2024) 112274. <https://doi.org/10.1016/j.jece.2024.112274>
25. H. Qi, W. Ren, X. Shi, Z. Sun, *Sep. Purif. Technol.*, 299 (2022) 121724. <https://doi.org/10.1016/j.seppur.2022.121724>
26. T.T.T. Trang, D.T. Huong, N.T.D. Nguyen, N.T. Dung, *Tạp chí Môi trường*, (9 năm 2022).